A Monte Carlo method for calculating the angle factor of diffuse cavities

2012 Metrologia 49 572

(http://iopscience.iop.org/0026-1394/49/4/572)

Metrologia **49** (2012) 572–576 doi:10.1088/0026-1394/49/4/572

A Monte Carlo method for calculating the angle factor of diffuse cavities

Qianqian Fang[1,2], Wei Fang[1], Zhenling Yang[1], Bing Xi Yu[1] and Hongbin Hu[1,2]

[1] Changchun Institute of Optics, Fine Mechanics and Physics, Chinese Academy of Science, Changchun 130033, People's Republic of China
[2] Graduate University of Chinese Academy of Science, Beijing 100049, People's Republic of China

Received 20 December 2011, in final form 28 May 2012
Published 5 July 2012
Online at stacks.iop.org/Met/49/572

Abstract
A Monte Carlo method is developed for computing the angle factors of diffuse cavities. It was confirmed that the Monte Carlo method for calculating angle factors is powerful and flexible due to its applicability to arbitrarily shaped cavities whose internal surfaces are diffuse. The algorithms of angle factors for regular shapes of cavities were first proposed. Then the calculations of angle factors for cavities with grooved cylinders were performed, and the reproducibility and correctness of the results obtained by the Monte Carlo method were estimated. In short, the Monte Carlo algorithms are certainly simple and accurate for those intricately shaped cavities compared with the mathematical calculation used before.

1. Introduction

Effective emissivity is the main figure of merit for blackbody cavities that are widely used as standard radiation sources in radiometry and radiation thermometry. Until now, several methods such as theoretical calculations, experimental measurement and Monte Carlo methods have been developed to obtain the effective emissivity of blackbody cavities. It has been confirmed that the Monte Carlo method is much more powerful and flexible than any other method [1–3].

Angle factors of diffuse cavities are very important in the process of calculating effective emissivity by the Monte Carlo method [4–6]. Sapritsky [4] and Heinisch [5] proposed that initially each ray was assigned a statistical weight of unity in the ray-tracing process, then this was multiplied by following every reflection and after each diffuse reflection, the statistical weight of the ray was reduced to take account of radiation loss through the cavity aperture, and that was defined by applying the angle factor between an element of the wall area at the point of reflection and the cavity aperture.

For diffuse reflection or emission, the spatial distribution of radiant intensity is

$$i_\theta = \mathrm{i_N} \cos\theta. \tag{1}$$

As shown in figure 1, i_N is the radiant intensity, which represents the radiant energy per unit time leaving a given surface $\mathrm{d}A$ in the direction normal to the diffuse wall and contained within unit solid angle. i_θ is the radiant intensity in the direction θ.

For diffuse cavities, if Ω_a is the solid angle subtended by the aperture when viewed from point ξ, then the angle factor F (the fraction of radiant energy leaving ξ that passes through the aperture) is

$$F(\xi) = \int_{\Omega_\mathrm{a}} i_\mathrm{N} \cos\theta_\xi \,\mathrm{d}\Omega \Big/ \int_{2\pi} i_\mathrm{N} \cos\theta_\xi \,\mathrm{d}\Omega, \tag{2}$$

where i_N is a constant. With this and with the introduction of $\mathrm{d}\Omega = \sin\theta_\xi \,\mathrm{d}\theta_\xi \,\mathrm{d}\phi$, equation (2) becomes

$$F(\xi) = \frac{1}{\pi} \int_{\Omega_\mathrm{a}} \cos\theta_\xi \,\mathrm{d}\Omega, \tag{3}$$

where θ_ξ is the angle between the normal to the cavity wall at $\vec{\xi}$ and the direction of the axis of an element of the solid angle $\mathrm{d}\Omega$.

Some researchers have used mathematical methods for its calculation. Sapritsky applied the superposition principle through angle factors between the cavity aperture and an element of the wall area, respectively either parallel or perpendicular to the aperture plane [7]. Heinisch [5] established a spherical coordinate system at the element of the wall area to reduce the dimension of integral equations.

Almost all the previous studies on angle factor of diffuse cavities have focused on mathematical analysis and

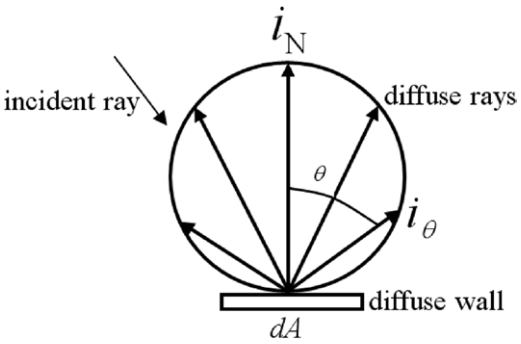

Figure 1. Spatial distribution of radiant intensity for diffuse reflection.

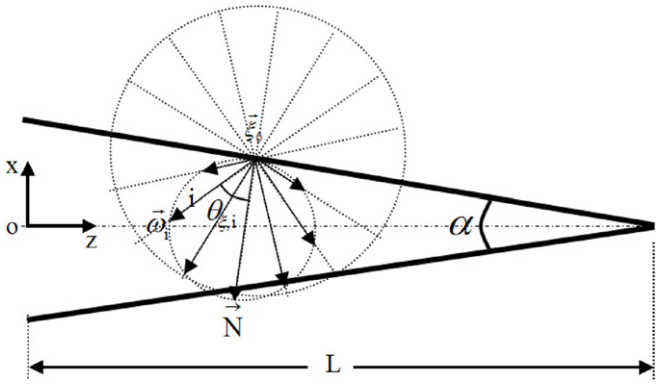

Figure 2. Conical cavity.

calculation. It is convenient for cavities with few surfaces such as cylindrical or conical cavities with smooth surfaces. As the number of surfaces increases, the complexity of the calculation grows rapidly. For some intricate shapes such as cylindrical or cylindro-conical cavities having a surface with grooves or screw threads, which are widely used as high-temperature blackbody furnaces for calibration of radiation thermometers [8–10], it is much more difficult to evaluate the angle factor accurately because of the complexity of the mathematical calculation.

In this paper, we develop a Monte Carlo method to calculate angle factors. The detailed algorithms for some regular shapes of cavities such as a cylinder, cone and cylindro-cone are first introduced. Then the angle factors of two types of grooved cylinder are evaluated. One is a rectangular groove and the other a triangular one whose reflective properties are diffuse.

2. Monte Carlo algorithm for regular shapes of cavities

2.1. The algorithm of diffuse directions

We apply an algorithm based on Marsaglia's algorithm [11] for generating points uniformly distributed on a spherical surface. The algorithm's key idea is that for perfectly diffuse reflection, the sphere with its centre at the cavity wall can be considered a uniform distribution of directions, like the big circle shown in figure 2, although there is a cosine relation of radiant intensity.

Generate pseudo-random numbers u_1 and u_2, independent and uniform on $(-1,1)$ until

$$S = u_1^2 + u_2^2 < 1. \tag{4}$$

Then form

$$\vec{\omega} = (\omega_x, \omega_y, \omega_z) = (2u_1(1-S)^{1/2}, 2u_2(1-S)^{1/2}, 1-2S). \tag{5}$$

Here $\vec{\omega}$ is the direction vector of unit length of a random ray. If $\vec{\xi}_0$ is the position vector of the ray's starting point, and $\Phi(\vec{\xi}_a) = 0$ is the equation describing the aperture plane, then it is easy to obtain the position vectors of intersection points where the rays, generated by $\vec{\xi}_0$, intersect with the aperture plane by solving the following system of equations:

$$\begin{aligned} \vec{\xi}_a &= \vec{\xi}_0 + \vec{\omega} t_a, \\ \Phi(\vec{\xi}_a) &= 0, \end{aligned} \tag{6}$$

where t_a is a parameter.

The position vectors of the intersection points are

$$\vec{\xi}_a = (x_a, y_a, z_a) = (x_0 + \omega_x t_a, y_0 + \omega_y t_a, z_0 + \omega_z t_a). \tag{7}$$

The rays generated by $\vec{\xi}_0$ can pass through the aperture if they satisfy

$$\begin{aligned} (x_0 + \omega_x t_a)^2 + (y_0 + \omega_y t_a)^2 &< R^2, \\ t_a &> 0, \end{aligned} \tag{8}$$

where R is the radius of the aperture.

2.2. The algorithm of radiant intensity

The radiant intensity leaving $\vec{\xi}_0$ follows the cosine distribution, like the inscribed circle shown in figure 2. Ray i which is along $\vec{\omega}_i$ is generated randomly, and the radiant intensity in the direction of $\vec{\omega}_i$ is

$$i_{\omega_i} = i_N \cos\theta_{\xi_0,i}, \tag{9}$$

where i_{ω_i} is the radiant intensity along $\vec{\omega}_i$, $\theta_{\xi_0,i}$ is the angle between the normal direction at $\vec{\xi}_0$ and the random direction i. The value of $\cos\theta_{\xi_0,i}$ can be described as

$$\cos\theta_{\xi_0,i} = \frac{\vec{\omega}_i \cdot \vec{N}}{|\vec{\omega}_i| \cdot |\vec{N}|}, \tag{10}$$

where $\vec{N}$ is the normal vector at $\vec{\xi}_0$. Because both $\vec{\omega}_i$ and $\vec{N}$ are unit vectors, equation (10) becomes

$$\cos\theta_{\xi_0,i} = \vec{\omega}_i \cdot \vec{N}. \tag{11}$$

For the sake of simplicity, the radiant intensity along $\vec{N}$ is assumed to be 1, and then the radiant intensity along $\vec{\omega}_i$ is $\cos\theta_{\xi_0,i}$. Because the rays generated by Marsaglia's algorithm are distributed over a spherical space, for the rays which are on the outer side of the cavity walls, the values of $\cos\theta_{\xi_0,i}$

are negative. So the radiant intensity of a random ray can be recorded as $|\cos\theta_{\xi_0,i}|$.

If there are N rays generated by $\vec{\xi}_0$ in all, and each ray has different radiant intensity $|\cos\theta_{\xi_0,i}|$ according to $\theta_{\xi_0,i}$ which is the angle between the normal direction at $\vec{\xi}_0$ and a random direction i, just n rays can pass through the aperture. Then the angle factor is

$$F(\xi_0) = \frac{2\sum_{i=1}^{n}\cos\theta_{\xi_0,i}}{\sum_{i=1}^{N}|\cos\theta_{\xi_0,i}|}. \tag{12}$$

Actually the radiation of a point located on the cavity wall is distributed over a hemispherical space instead of a spherical space, so there is a factor 2 in formula (12). For obtaining one value of angle factor, we chose 10^6 rays in the calculations to ensure calculation accuracy. In order to verify the correctness of the Monte Carlo method, we chose a conical cavity in figure 2 whose angle factors can be easily calculated by mathematical calculations.

For the conical cavity with $\alpha = 30^\circ$, $L = 10$. F was calculated at 1000 points which are located on the cavity walls and uniformly distributed along the z-axis in the range $0 \leqslant z \leqslant L$ by the Monte Carlo method and mathematical formulae [7], respectively. The results of the two methods are in very good agreement with each other. The discrepancies of the results follow a normal distribution and the median discrepancy is 1.3×10^{-5} (95% confidence interval: -1.0×10^{-5}–3.6×10^{-5}).

3. Monte Carlo algorithm for cavities with grooved cylinders

Because of ease and economy of construction, cylindrical or cylindro-conical cavities having a surface with grooves or screw threads are widely used. However, it is much more difficult to evaluate the angle factor accurately because of the complexity of the shapes.

Calculations for the angle factors of cavities with grooved cylinders were performed. In figures 3 and 4, two kinds of cylindro-conical cavities are illustrated schematically. Figures 3(*a*) and 4(*a*) represent a cavity with a rectangular-grooved cylinder and a triangular-grooved cylinder, respectively. For the sake of simplicity, we set $\Delta = 1$, $R = 5$ throughout, and establish the uniform Cartesian coordinate system. The xy plane is coincident with the aperture plane, and the z-axis is along the direction of cavity length.

3.1. Results of a cavity with a rectangular-grooved cylinder

The rectangular-grooved cylinder is periodically repeated along the z-axis, and the length of the cycle is 2. In figure 3(*a*), one cycle is specially shown with each surface marked with different letters (A, B, C and D). Different algorithms are adopted for marked surfaces as follows.

(A) For $\vec{\xi}_0$ on surface A, the situation is the same as regular cavities. Diffuse directions are generated by Marsaglia's algorithm. The radiant intensities satisfy the cosine relation as formula (9). The rays generated by $\vec{\xi}_0$ can escape from the cavity directly if they satisfy formula (8). Finally, we can get the angle factor at $\vec{\xi}_0$ by formula (12).

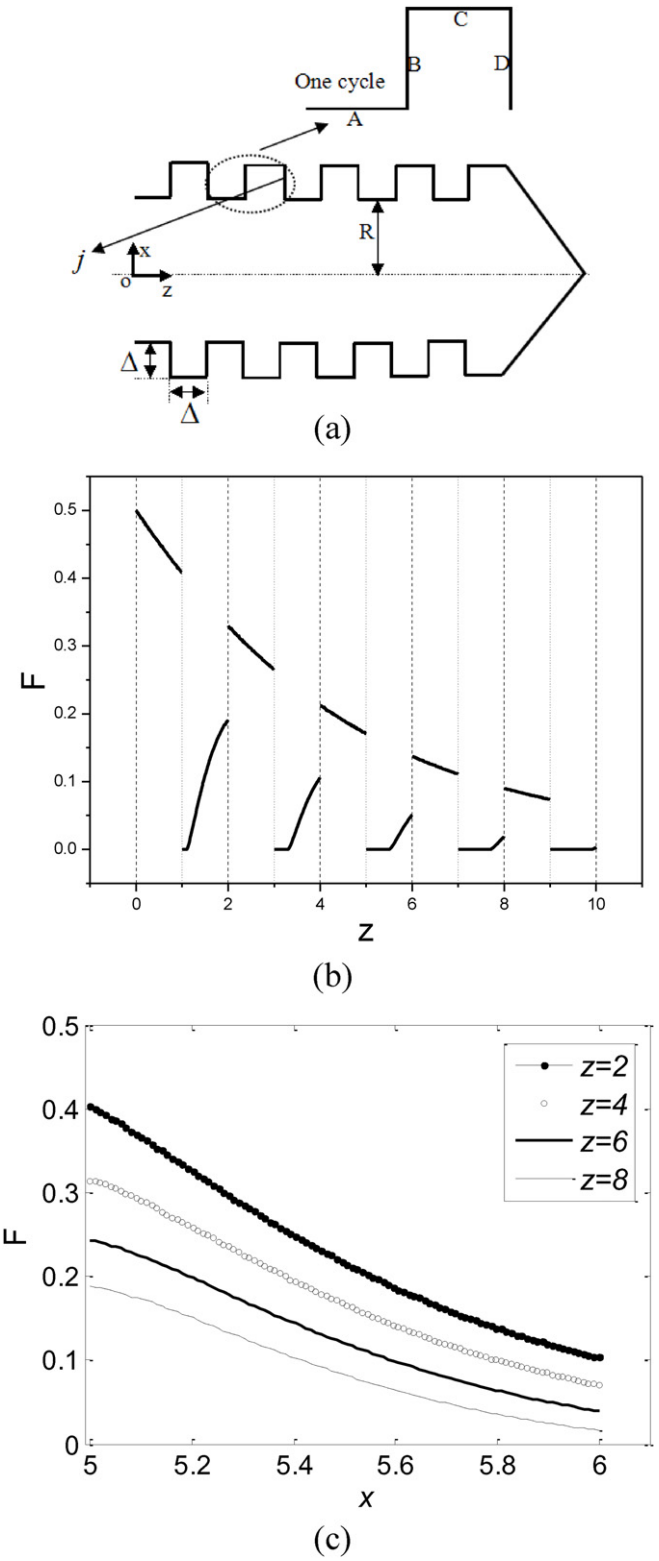

Figure 3. (*a*) Cavity with a rectangular-grooved cylinder; (*b*) angle factors as a function of the z-axis; (*c*) angle factors as a function of the x-axis.

(B) For $\vec{\xi}_0$ on surface B, there are no rays escaping from the cavity directly. So the angle factors are equal to 0.

(C) For $\vec{\xi}_0$ on surface C or D, according to formula (8), ray j starting from $\vec{\xi}_0$ located on surface D can pass through the

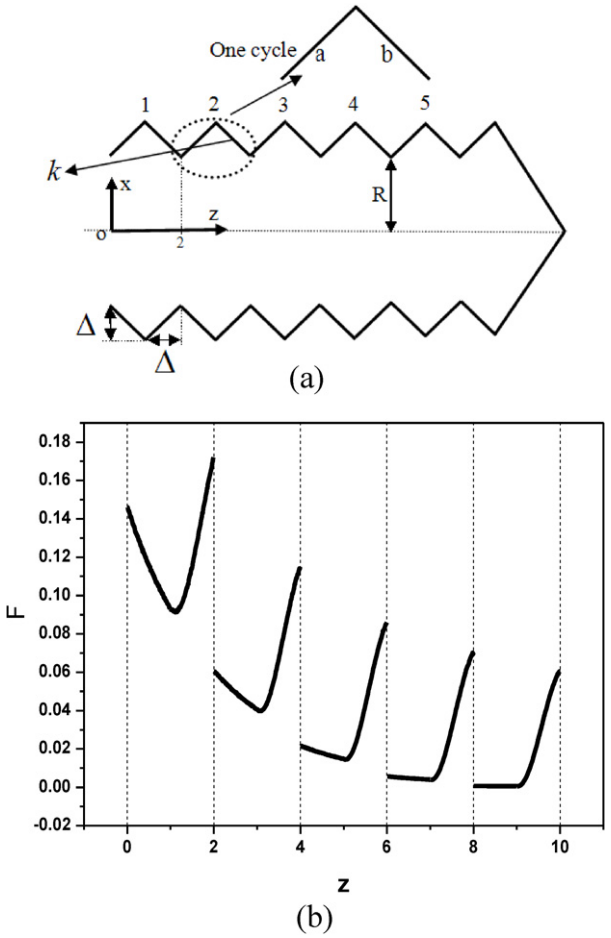

Figure 4. (*a*) Cavity with a triangular-grooved cylinder; (*b*) angle factors as a function of the z-axis.

cavity. However, the ray is stopped by surface B of the same cycle before it escapes from the cavity as figure 3(*a*) shows.

We can get the intersection points $\vec{\xi}_a$ of the rays and the aperture plane by solving the following system of equations:

$$\begin{aligned} z_a &= 0, \\ \vec{\xi}_a &= \vec{\xi}_0 + \vec{\omega} t_a, \end{aligned} \tag{13}$$

where $z_a = 0$ represents the equation of the aperture plane, and t_a is a parameter.

The intersection points $\vec{\xi}'$ of the rays and surface B, which is in the same cycle with $\vec{\xi}_0$, can be solved by the following system of equations:

$$\begin{aligned} z' &= Z_1 - 1, \\ \vec{\xi}' &= \vec{\xi}_0 + \vec{\omega} t' \end{aligned} \tag{14}$$

where $z' = Z_1 - 1$ represents the plane equation of surface B, which is in the same cycle with $\vec{\xi}_0$. Z_1 is the minimal integer larger than z_0 and t' is a parameter.

By solving systems of equations (13) and (14), $\vec{\xi}_a$ and $\vec{\xi}'$ can be described as follows:

$$\begin{aligned} \vec{\xi}_a &= (x_a, y_a, z_a) = (x_0 + \omega_x t_a, y_0 + \omega_y t_a, z_0 + \omega_z t_a), \\ \vec{\xi}' &= (x', y', z') = (x_0 + \omega_x t', y_0 + \omega_y t', z_0 + \omega_z t'), \end{aligned} \tag{15}$$

If $\vec{\xi}_a$ and $\vec{\xi}'$ satisfy

$$\begin{aligned} (x_0 + \omega_x t_a)^2 + (y_0 + \omega_y t_a)^2 &< R^2, \\ (x_0 + \omega_x t')^2 + (y_0 + \omega_y t')^2 &< R^2, \\ t_a &> 0, \\ t' &> 0, \end{aligned} \tag{16}$$

then it indicates the rays can pass through the aperture. Finally, the angle factor can be calculated by formula (12).

Figure 3(*b*) gives the angle factor distribution for the rectangular-grooved cylinder as a function of z in the range $0 < z < 10$. The angle factor of surface A decreases with increasing z. The angle factor of surface C has a great increase in the same cycle, while for the points located on the same position of different cycles, the angle factor decreases with increasing z. It is also obvious that the angle factor curve is not continuous at inflection points.

For the points on surface B, the angle factors are equal to 0 and remain constant. However, the situation is different for the points located on surface D. The angle factors of surface D in four different cycles are calculated. The curves of angle factors as a function of x in the range $5 < x < 6$ (at $z = 2$, 4, 6 and 8) are shown in figure 3(*c*). The angle factor decreases with increasing x for the points located on the same surface while for the points located at the same position of different cycles, it is obvious that the angle factors are much larger for the points that are closer to the cavity aperture.

3.2. Results of a cavity with a triangular-grooved cylinder

As in figure 4(*a*), the triangular-grooved cylinder is periodically repeated along the z-axis. Five complete cycles are numbered. The second cycle is specially shown with two surfaces marked with different letters (a and b). The rays generated by $\vec{\xi}_0$ which is located on surface a or b may be stopped by some surface before passing through the aperture. For example, it appears that ray k starting from $\vec{\xi}_0$ located on surface b in the second cycle can pass through the cavity according to formula (8). However, the ray is stopped by the plane ($z = 2$) before it escapes from the cavity. If $\vec{\xi}_0$ is in the m cycle of the triangular-grooved cylinder cavity, we can get the intersection points $\vec{\xi}_a$ of the rays and the aperture plane by equation (13), and the intersection points $\vec{\xi}''$ of the rays and the plane ($z = 2(m-1)$) by the following system of equations:

$$\begin{aligned} z'' &= 2(m-1), \\ \vec{\xi}'' &= \vec{\xi}_0 + \vec{\omega} t'', \end{aligned} \tag{17}$$

where m is the minimal integer larger than $z_0/2$, t_a and t'' are parameters.

By solving the system of equations (13) and (17), $\vec{\xi}_a$ and $\vec{\xi}''$ can be described as follows:

$$\begin{aligned} \vec{\xi}_a &= (x_a, y_a, z_a) = (x_0 + \omega_x t_a, y_0 + \omega_y t_a, z_0 + \omega_z t_a), \\ \vec{\xi}'' &= (x'', y'', z'') = (x_0 + \omega_x t'', y_0 + \omega_y t'', z_0 + \omega_z t''). \end{aligned} \tag{18}$$

If $\vec{\xi}_a$ and $\vec{\xi}''$ satisfy

$$\begin{aligned}(x_0 + \omega_x t_a)^2 + (y_0 + \omega_y t_a)^2 < R^2,\\ (x_0 + \omega_x t'')^2 + (y_0 + \omega_y t'')^2 < R^2,\\ t_a > 0,\\ t'' > 0,\end{aligned} \tag{19}$$

then it indicates the rays can pass through the aperture. Finally, the angle factor can be calculated by formula (12).

Figure 4(*b*) expresses the angle factor distribution as a function of z in the range $0 < z < 10$. The angle factor of surface a decreases with increasing z. The angle factor of surface b increases significantly in the same cycle with z, while for the points located at the same position of different cycles, the angle factor decreases with increasing z. The curve is continuous in the same cycle, but discontinuous at connections of different cycles.

3.3. Uncertainty of the results by the Monte Carlo method

In order to estimate the reproducibility and correctness of the results of grooved cylinders obtained by the Monte Carlo method, we calculated the uncertainty of the results. Firstly, for a random point located on the cavity wall, repeated calculations by the Monte Carlo method were performed in order to estimate the reproducibility of the results. And then the discrepancies of the results obtained by the Monte Carlo method and mathematical method were used to estimate the correctness of the results.

A point was generated randomly on the rectangular-grooved cavity wall, as well as the triangular-grooved one. The angle factors of the two points were calculated 1000 times by the Monte Carlo method. The standard deviation of the results is 3.1×10^{-4} (95% confidence interval: 2.9×10^{-4}–3.3×10^{-4}) for the point located on the rectangular-grooved cavity and 1.5×10^{-4} (95% confidence interval: 1.4×10^{-4}–1.7×10^{-4}) for the point located on the triangular-grooved one.

For the two kinds of grooved cavities, angle factors were calculated at 1000 points, which are located on the walls of the cavities and uniformly distributed along the z-axis in the range $0 < z < 10$ by the Monte Carlo method and the method proposed by Heinisch [5] of solving integral formula (3), respectively. The results of the two methods are in good agreement. The discrepancies of the results of the two methods follow a normal distribution and the median discrepancies are -7×10^{-6} (95% confidence interval: -3.2×10^{-5}–1.8×10^{-5}) for the rectangular-grooved cavity and 1.6×10^{-5} (95% confidence interval: -1.1×10^{-5}–4.2×10^{-5}) for the triangular-grooved one.

4. Conclusion

The Monte Carlo method for calculating the angle factors of diffuse cavities can not only give accurate results, but is more powerful, flexible and convenient. This is due to its applicability to arbitrarily shaped cavities whose internal surfaces are diffuse. In this paper we find that the Monte Carlo method can be successfully applied to a variety of cavities. Whether it is a regular cavity or a combination of complex structure (with grooves), the algorithms are very simple and easy to understand.

The algorithms are implemented in a program working on a PC under a 32-bit MS Windows operating system. For obtaining one effective angle factor value, 10^6 rays are emitted from $\vec{\xi}_0$ to ensure calculation accuracy, and it just takes tens of seconds. Overall, whether in precision or the simplicity of algorithms, the Monte Carlo method for calculating the angle factors of diffuse cavities is excellent.

References

[1] Prokhorov A V 1998 Monte Carlo method in optical radiometry *Metrologia* **35** 465–71

[2] Ono A 1980 Calculation of the directional emissivities of cavities by the Monte Carlo method *J. Opt. Soc. Am.* **70** 547–54

[3] Prokhorov A V and Hanssen L M 2004 Effective emissivity of a cylindrical cavity with an inclined bottom: I. Isothermal cavity *Metrologia* **41** 421–31

[4] Sapritsky V I and Prokhorov A V 1992 Calculation of the effective emissivities of specular-diffuse cavities by the Monte Carlo method *Metrologia* **29** 9–14

[5] Heinisch R P, Sparrow E M and Shamsundar N 1973 Radiant emission from baffled conical cavities *J. Opt. Soc. Am.* **63** 152–8

[6] Sapritsky V I and Prokhorov A V 1995 Spectral effective emissivities of non-isothermal cavities calculated by the Monte Carlo method *Appl. Opt.* **34** 5645–52

[7] Siegel R and Howell J R 2002 *Thermal Radiation Heat Transfer* vol 1 (London: Taylor and Francis)

[8] Blevin W R and Brown W J 1971 A precise measurement of the Stefan–Boltzmann constant *Metrologia* **7** 15–29

[9] Coates P B and Andrews J W 1978 A precise determination of the freezing point of copper *J. Phys. F: Met. Phys.* **8** 277–85

[10] Quinn T J 1980 Emissivity of near blackbody cavities for high-temperature pyrometry *High Temp. High Pressures* **12** 359–72

[11] Marsaglia G 1972 Choosing a point from the surface of a sphere *Ann. Math. Stat.* **43** 645–6